Studies on the mechanism of general anesthesia.

Mahmud Arif Pavel[1,2], E. Nicholas Petersen[1,2], Richard A. Lerner[3], and Scott B. Hansen[1,2,*]

[1]Department of Molecular Medicine, [2]Department of Neuroscience, The Scripps Research Institute, Jupiter, Florida 33458, USA.

[3]Department of Chemistry, The Scripps Research Institute, La Jolla, California 92037, USA

*Correspondence: shansen@scripps.edu

ABSTRACT

Inhaled anesthetics are a chemically diverse collection of hydrophobic molecules that robustly activate TWIK related K+ channels (TREK-1) and reversibly induce loss of consciousness. For a hundred years anesthetics were speculated to target cellular membranes, yet no plausible mechanism emerged to explain a membrane effect on ion channels. Here we show that inhaled anesthetics (chloroform and isoflurane) activate TREK-1 channels through disruption of ordered lipid domains (rafts). Super resolution imaging shows anesthetic raft disruption expels the enzyme phospholipase D2 (PLD2), activating TREK-1. Catalytically dead PLD2 robustly blocks anesthetic specific TREK-1 currents in whole cell patch-clamp. Addition of a PLD2 binding-site renders the anesthetic-insensitive TRAAK channel sensitive. General anesthetics chloroform, isoflurane, diethyl ether, xenon, and propofol all activate PLD2 in cellular membranes. Our results suggest a two-step model of anesthetic TREK-1 activation. First, inhaled anesthetics disrupt lipid rafts. Second, translocation and PLD2-dependent production of anionic lipid activates TREK-1.

INTRODUCTION

In 1846 William Morton demonstrated general anesthesia with inhaled anesthetic diethyl ether[1]. For many anesthetics (but not all), lipophilicity is the single most significant indicator of potency; this observation is known as the Overton-Mayer correlation[2,3]. This correlation, named for its discoverers in the late 1800's, and the chemical diversity of anesthetics (Supplementary Fig. S1a) drove anesthetic research to focus on perturbations to membranes as a primary mediator of inhaled anesthesia[3]. Over the last two decades evidence suggests that anesthetics can act through direct binding to ion channels,[4] but many properties of anesthesia remain unexplained[5], and plausible roles[6] for the membrane have yet to be established experimentally.

Given the decades-long controversies and conflicting data, we hypothesized that some anesthetics act through an indirect membrane route. Our hypothesis is supported by the fact that enantiomers of the analgesic toxin GsMTx4D[7,8] behave identically in modulating ion channels[9], thereby largely precluding that their target is chiral. Thus, from a chemical point of view, targets such as lipids with large achiral components, rather than chiral targets such as proteins, would be a preferred initial target. Other agents that could act through a non-direct route include the inhaled (volatile) anesthetic xenon, which is a hydrophobic atom, and small, achiral molecules such as diethyl ether, chloroform, and halothane.

TREK-1 is an anesthetic-sensitive two-pore-domain potassium (K2P) channel. Xenon, diethyl ether, halothane, and chloroform robustly activate TREK-1 at clinical concentrations[10,11] and genetic deletion of TREK-1 decreases anesthesia sensitivity in mice[12]. Importantly, GsMTx4D also activates TREK-1[8]. Since this activation is indirect[9], we reasoned inhaled anesthetics could also activate through an indirect route, but how?

In 1997 a theory emerged suggesting that disruption of ordered lipids surrounding a channel could activate the channel[13]. Disruption of ordered lipids (now commonly referred to as lipid

rafts[14]) allows proteins to translocate out of the raft and experience a new chemical environment[15] (Supplementary Fig. S1b-c). If inhaled anesthetics can disrupt lipid rafts to activate a channel, this would constitute a mechanism distinct from the usual receptor-ligand interaction and establish a definitive membrane mediated mechanism for an anesthetic. Here we show inhaled anesthetics disrupt lipid rafts in the membranes of cultured neuronal and muscle cells. Anesthetic disruption of rafts then releases lipid activators which activate TREK-1 channels. This result suggests that researchers should consider indirect mechanisms when studying the effect of anesthetics on ion channels.

Anesthetic disruption of lipid rafts (GM1 domains)

The best studied raft domains contain saturated lipids cholesterol and sphingomyelin (e.g. monosialotetrahexosylganglioside1 (GM1)) (see Supplementary Fig. S1b-c)[14] and bind cholera toxin B (CtxB) with high affinity. Anesthetics lower the melting temperature and expand GM-1 domains in artificial membranes and membrane vesicles[16–18]. Lipid rafts are not visible in a light microscope and super-resolution imaging (e.g., direct stochastical optical reconstruction microscopy (dSTORM)) only recently made possible the observation of lipid rafts (20-200 nm) in cellular membranes[19–22], allowing us to test for the first time the hypothesis of raft disruption as a mechanism of anesthetic action on an ion channel.

To test raft (GM1 domain) disruption we treated N2A neuroblastoma cells with anesthetics chloroform or isoflurane (Fig. 1a-b) and C2C12 cells with chloroform (Supplementary Fig. S2c-d) at 1mM (a clinical concentration), and monitored fluorescent CtxB binding by dSTORM. Anesthetic strongly increased both the diameter (Fig. 1c; Supplementary Fig. S2e) and area (Fig. 1d; Supplementary Fig. S2f) of GM1 domains (Fig. 1b-d) in the cell membrane. The Ripley's radius, a measure of space between domains, decreased dramatically for both chloroform and isoflurane suggesting the domains expand[23] and possibly divide (Supplementary

Fig. S2a, Fig. 1f). Methyl-β-cyclodextrin (MβCD), a chemical that disrupts GM1 domains by removing cholesterol[15], reduced the total number of domains 55% to 285 ± 42 per cell (mean ± SEM, n=10). Binning the domains into small (0-150 nm) and large (150-500nm) revealed a clear shift from small to large domains in the presence of inhaled anesthetics and revealed the opposite effect after MβCD treatment (Supplementary Fig. S2b).

Mechanism of anesthetic sensitivity in TREK-1 channels

To distinguish the contribution of a putative indirect anesthetic effect from a direct one, we first tested the contribution of direct binding to TREK-1 anesthetic sensitivity in a flux assay and found no evidence for direct binding (Supplementary Fig. S3a). The most definitive experiment to show a channel is directly modulated by a ligand is to purify and functionally reconstitute the channel into lipid vesicle of known composition. Ion channels are now routinely expressed and purified and assayed in vesicles. Purified channels robustly recapitulate small molecules binding to channels in a cell free system using a flux assay[24] and in detergent[25]. We functionally reconstituted purified TREK-1 into 16:1 phosphatidylcholine (PC) with 18:1 phosphatidylglycerol (PG) (85:15 mol% ratio) liposomes and we found that neither chloroform nor isoflurane (1 mM, a clinically relevant concentration) had a direct effect on TREK-1 activity (Supplementary Fig. S3a-b). Changing the lipids and ratios to 18:1PC/18:1PG (90/10 mol%)[25] also had no effect (data not shown).

To assure that the channel was properly reconstituted and in conditions capable of increased potassium flux, we reconstituted a mutant TREK-1 with double cysteines that allosterically induced TREK-1 activation[25,26]. Compared to the open TREK-1 control, inhaled anesthetics failed to activate TREK-1 (Supplementary Fig. S3a-b). This result is inconsistent with direct

binding of anesthetics as the primary mechanism and lead us to consider an indirect mechanism of TREK-1 activation.

Activation of TREK-1 by inhaled anesthetics, was previously shown to require a disordered loop in the channel's C-terminus[10] (Supplementary Fig. S3e). The enzyme phospholipase D2 (PLD2) also binds to and activates through same C-terminal region in TREK-1[27]. We recently showed disruption of rafts (GM1 domains) by mechanical force activates PLD2 by substrate presentation—the enzyme translocated out of rafts to disordered lipids and substrate[15]. If anesthetics disrupt GM1 domains then we expect PLD2 to translocate and activate TREK-1, leading us to hypothesize that raft disruption may be responsible for the anesthetic sensitivity observed in TREK-1 channels.

To test the contribution of raft disruption to TREK-1 anesthetic sensitivity, we applied chloroform to HEK293 cells expressing TREK-1 and a catalytically dead K758R PLD2 mutant (xPLD2) that blocks anionic lipid (e.g. PA and PG) production[28]. We found xPLD2 blocked all detectible chloroform specific current (Fig 2a-c). This result suggests a two-step mechanism for anesthetic action on TREK-1 channels. First, anesthetics disrupt GM1 domains releasing PLD2 and second, the enzyme binds to the C-terminus and activates the channel through increased local concentration of anionic lipid (Fig 2d). The lack of TREK-1 current in the presence of anesthetic further confirms our flux assay, i.e. direct binding of anesthetic is insufficient to activate the channel absent PLD2 activity.

TRAAK is an anesthetic insensitive homolog of TREK-1. Interestingly, native TRAAK is also insensitive to PLD2[27]. However, concatenating PLD2 to the N-terminus maximally activates TRAAK and introduction of the PLD2 binding domain from TREK-1 renders TRAAK PLD2 sensitive[27]. If PLD2 is responsible for anesthetic sensitivity in TREK-1, we reasoned we could

render TRAAK anesthetic sensitive by introducing the PLD2 binding site into the C-terminus of TRAAK (Fig. 3a).

We over expressed the previously characterized PLD2 sensitive TRAAK chimera[27] (TRAAK/ctTREK) in HEK cells. As expected, in the presence of 1mM chloroform, TRAAK/ctTREK robustly responded to chloroform (Fig. 3b,d). To confirm the response is due to PLD2 localization and not a direct interaction of the anesthetic with a structural feature of the TREK-1 C-terminus, we over expressed the chimera with xPLD2 and found chloroform had no effect on the channel. This result suggests the disordered C-terminus exerts its anesthetic effect through binding to PLD2 and not direct binding of anesthetic to the C-terminus (Fig. 3e).

Anesthetics displace PLD2 out of GM1 rafts.

To confirm our two-step mechanism, we directly imaged PLD2 translocation out of lipid rafts using dSTORM. Palmitoylation localizes proteins to rafts[29] including many ion channels[30]. TREK-1 is not palmitoylated, but palmitoylation could sequester PLD2 away from TREK-1[15] (Supplementary Fig. S1b-c).

Treating the N2A cells with chloroform or isoflurane (1 mM), caused PLD2 to translocate out of GM1 domains (Fig 4a). We verified translocation by cross correlation analysis—PLD2 strongly associated with GM1 domains prior to treatment (Fig 4b, grey trace) but only weak association after treatment with anesthetic (green traces). The anesthetic-induced translocation of PLD2 as depicted in Fig. 4d was significant and similar in magnitude to MβCD stimulated translocation (Fig. 2b-c). The PLD2 translocation confirms that anesthetic expansion of GM-1 domains is indeed a form of domain disruption. We obtained similar results in C2C12 cells with chloroform (Supplementary Fig. S4).

Anesthetics activate PLD2 through raft disruption.

If raft disruption is a general mechanism for anesthetics then all known activators of TREK-1 should also activate PLD2. We tested enzymatic activation of PLD2 by treating live cells with a spectrum of chemically diverse inhaled anesthetics and monitoring activity using an assay that couples choline release to a fluorescent signal[15] (Fig. 5a-d). Diethyl ether, chloroform, isoflurane, and xenon all significantly activated PLD2 (Fig. 5g). Isoflurane had the greatest effect (Fig. 5g) in N2A cells and chloroform had the greatest effect among inhaled anesthetics in C2C12 myoblast cells (Supplementary Fig. S5b,f). This activation suggests anesthetic disruption of GM1 domains allows PLD to access substrate and catalyze the production of anionic signaling lipids (e.g. PA and PG) — a result similar to PLD2's activation by mechanical disruption of GM1 domains[15]. Ketamine, an injectable NMDA receptor specific anesthetic[31] had no effect on PLD activity, as expected for a direct ligand-protein interaction (Fig. 5f,g).

We also tested the injectable general anesthetics propofol[4]. Surprisingly, propofol robustly activated PLD2 in N2A cells (Fig. 5d,g). If our mechanism is correct, then propofol should lead to TREK-1 activation. As predicted, propofol (50 μM), robustly increased TREK-1 currents (Fig 5h) in whole cell patch-clamp. Propofol's effect was significant (Fig. 5j, $p=0.017$, two tailed Student's t test,) and co-transfection of xPLD2 with TREK-1 completely blocked the propofol specific current. Hence, PLD2 activity predicts channel function and this result suggests propofol works through the same pathway as inhaled anesthetics to activate TREK-1. In C2C12 cells, PLD2 activation required 400 μM concentrations of propofol suggesting cell specific regulation of raft disruption or PLD2 translocation (Supplementary Fig. S5d,f).

DISCUSSION

We conclude inhaled anesthetics (at clinical concentrations) primarily disrupt GM1 domains to elicit a response in TREK-1 channels. Anesthetics clearly disrupt the rafts, release PLD2, which

then binds to TREK-1 and increases the local concentration of anionic signaling lipid in the membrane to activate TREK-1. Our proposed model is consistent with known properties of inhaled anesthetics (summarized in Supplementary Fig. S5c-d), specifically perturbation to TREK-1 are through PLD2 and lipid binding sites[10,11,32]. The binding of PLD upon release from a lipid nanodomain nicely explains how the C-terminus renders a channel anesthetic sensitive when the domain is highly charged, devoid of structure, and has no obvious hydrophobicity expected to bind an anesthetic (Supplementary Fig. S5c-d).

Anesthetic disruption of GM1 domains likely affects many proteins, including many ion channels, as palmitoylation alone is sufficient to target proteins to GM1 domains[29]; and many ion channels are palmitoylated[30]. In theory, domain disruption could directly cause translocation of a palmitoylated channel in a single step, exposing the channel to activating lipid as originally proposed[13]. We chose a two-step system with PLD to avoid potential confounding effects on the transmembrane domain of the channel, e.g., palmitoylation is unlikely to sense changes in bilayer thickness. Many important signaling molecules are palmitoylated including tyrosine kinases, GTPases, CD4/8, and almost all G-protein alpha subunits[33]. Displacement of these proteins from lipid rafts could alter their available substrates and affect downstream singling, likely contributing to the overall anesthetic state of a cell.

At least three factors could influence the sensitivity/selectivity of TREK-1 to anesthetic disruption; 1) the type of PLD2 lipidation, 2) regulation of the PLD2 affinity for the C-terminus, and 3) the cellular regulation of raft domain integrity. For example, the affinity of PLD2 to the C-terminus could be affected by phosphorylation. A decreased affinity would disfavor translocation and reduce sensitivity to anesthetic. Removal of a palmitate from PLD2 or replacing a palmitate with a myristate should decrease raft localization and increase anesthetic sensitivity. Alternatively, if the cell were to decrease desaturase activity or upregulate cholesterol and

saturated lipids, these changes would increase PLD2 localization to rafts and decrease the sensitivity of TREK-1 to anesthetic. The anesthetic sensitivity of TASK channels, a homolog of TREK-1, is likely governed by these principles since swapping the C-terminus of TASK for TREK-1 also swaps the anesthetic sensitivity[10].

Lastly, we considered the biophysical effect of anesthetics on the bulk membranes or 'non-raft' membranes. We saw very little effect of clinical concentration of anesthetics on TREK-1 reconstituted into (DOPC) liposomes in our flux assay (Supplementary Fig. 3a-b), a mimic of bulk lipids. This result agrees with previous studies that showed the effect of anesthetics on bulk lipids is insufficient to activate a channel[34] at clinical concentrations despite the fact that anesthetics fluidize and thin membranes[35]. TREK-1 is very sensitive to membrane thickness (Nayebosadri unpublished data). It's possible we failed to test an optimal thickness that is responsive in artificial systems, however, the fact that xPLD2 blocked all detectible anesthetic currents in whole cells suggests, in a biological membrane, domain disruption and PLD2 translocation is the primary mechanism for anesthetic activation of TREK-1, not thinning of bulk lipids. Our domain disruption mechanism does not preclude an anesthetic binding directly to channels[2,4,36]. For example, local anesthetics inhibit TREK-1 through a distinct mechanism (Pavel unpublished data).

Our data show anionic lipids are central mediators of anesthetic action on ion channels and these results suggest lipid regulatory molecules and lipid binding sites in channels may be effective targets for treating nervous system disorders and understanding the thresholds that govern intrinsic nerve cell excitability. Thus the system we describe here obviously did not evolve to interact with diethyl ether and a search as to what the endogenous analogue that activates this physiological system is warranted.

REFERENCES

1. Seutin, V. M. Mechanisms of actions of inhaled anesthetics. *N. Engl. J. Med.* **349,** 909-910-910 (2003).
2. Urban, B. W., Bleckwenn, M. & Barann, M. Interactions of anesthetics with their targets: Non-specific, specific or both? *Pharmacol. Ther.* **111,** 729–770 (2006).
3. Kopp Lugli, A., Yost, C. S. & Kindler, C. H. Anaesthetic mechanisms: update on the challenge of unravelling the mystery of anaesthesia. *Eur. J. Anaesthesiol.* **26,** 807–20 (2009).
4. Franks, N. P. General anaesthesia: from molecular targets to neuronal pathways of sleep and arousal. *Nat. Rev. Neurosci.* **9,** 370–86 (2008).
5. Sonner, J. M. A hypothesis on the origin and evolution of the response to inhaled anesthetics. *Anesth. Analg.* **107,** 849–54 (2008).
6. Lynch, C. Meyer and Overton revisited. *Anesth. Analg.* **107,** 864–7 (2008).
7. Pyo, S. *et al.* A tarantula spider toxin , GsMTx4 , reduces mechanical and neuropathic pain. **137,** 208–217 (2008).
8. Gnanasambandam, R. *et al.* GsMTx4: Mechanism of Inhibiting Mechanosensitive Ion Channels. *Biophys. J.* **112,** 31–45 (2017).
9. Suchyna, T. M. *et al.* Bilayer-dependent inhibition of mechanosensitive channels by neuroactive peptide enantiomers. *Nature* **430,** 235–240 (2004).
10. Patel, a J. *et al.* Inhalational anesthetics activate two-pore-domain background K+ channels. *Nat. Neurosci.* **2,** 422–6 (1999).
11. Gruss, M. *et al.* Two-pore-domain K+ channels are a novel target for the anesthetic gases xenon, nitrous oxide, and cyclopropane. *Mol Pharmacol* **65,** 443–452 (2004).
12. Heurteaux, C. *et al.* TREK-1, a K+ channel involved in neuroprotection and general anesthesia. *EMBO J.* **23,** 2684–2695 (2004).
13. Lerner, R. A. A hypothesis about the endogenous analogue of general anesthesia. *Proc*

Natl Acad Sci U S A **94,** 13375–13377 (1997).

14. Lingwood, D. & Simons, K. Lipid rafts as a membrane-organizing principle. *Science* **327,** 46–50 (2010).

15. Petersen, E. N., Chung, H.-W., Nayebosadri, A. & Hansen, S. B. Kinetic disruption of lipid rafts is a mechanosensor for phospholipase D. *Nat. Commun.* **7,** 13873 (2016).

16. Gray, E., Karslake, J., Machta, B. B. & Veatch, S. L. Liquid general anesthetics lower critical temperatures in plasma membrane vesicles. *Biophys. J.* **105,** 2751–9 (2013).

17. Papahadjopoulos, D., Jacobson, K., Poste, G. & Shepherd, G. Effects of local anesthetics on membrane properties. I. Changes in the fluidity of phospholipid bilayers. *Biochim. Biophys. Acta* **394,** 504–19 (1975).

18. Lee, A. G. Model for action of local anaesthetics. *Nature* **262,** 545–8 (1976).

19. Jones, S. a, Shim, S.-H., He, J. & Zhuang, X. Fast, three-dimensional super-resolution imaging of live cells. *Nat. Methods* **8,** 499–508 (2011).

20. Huang, B., Wang, W., Bates, M. & Zhuang, X. Three-dimensional super-resolution imaging by stochastic optical reconstruction microscopy. *Science* **319,** 810–3 (2008).

21. Betzig, E. *et al.* Imaging intracellular fluorescent proteins at nanometer resolution. *Science* **313,** 1642–1645 (2006).

22. Hess, S. T., Girirajan, T. P. K. K. & Mason, M. D. Ultra-high resolution imaging by fluorescence photoactivation localization microscopy. *Biophys. J.* **91,** 4258–4272 (2006).

23. Kinnun, J. J., Bittman, R., Shaikh, S. R. & Wassall, S. R. DHA Modifies the Size and Composition of Raftlike Domains: A Solid-State2H NMR Study. *Biophys. J.* **114,** 380–391 (2018).

24. Su, Z., Brown, E. C., Wang, W. & MacKinnon, R. Novel cell-free high-throughput screening method for pharmacological tools targeting K+ channels. *Proc. Natl. Acad. Sci. U. S. A.* **113,** 1602815113- (2016).

25. Cabanos, C., Wang, M., Han, X. & Hansen, S. B. A Soluble Fluorescent Binding Assay

Reveals PIP2 Antagonism of TREK-1 Channels. *Cell Rep.* **20,** 1287–1294 (2017).

26. Brohawn, S. G., Campbell, E. B. & MacKinnon, R. Physical mechanism for gating and mechanosensitivity of the human TRAAK K+ channel. *Nature* **516,** 126–130 (2014).

27. Comoglio, Y. *et al.* Phospholipase D2 specifically regulates TREK potassium channels via direct interaction and local production of phosphatidic acid. *Proc. Natl. Acad. Sci. U. S. A.* **111,** 13547–52 (2014).

28. Sung, T. C. *et al.* Mutagenesis of phospholipase D defines a superfamily including a trans-Golgi viral protein required for poxvirus pathogenicity. *EMBO J.* **16,** 4519–30 (1997).

29. Levental, I., Lingwood, D., Grzybek, M., Coskun, U. & Simons, K. Palmitoylation regulates raft affinity for the majority of integral raft proteins. *Proc. Natl. Acad. Sci.* **107,** 22050–22054 (2010).

30. Shipston, M. J. Ion channel regulation by protein palmitoylation. *J. Biol. Chem.* **286,** 8709–8716 (2011).

31. MacDonald, J. F. *et al.* Actions of ketamine, phencyclidine and MK-801 on NMDA receptor currents in cultured mouse hippocampal neurones. *J. Physiol.* **432,** 483–508 (1991).

32. Bertaccini, E. J., Dickinson, R., Trudell, J. R. & Franks, N. P. Molecular modeling of a tandem two-pore-domain potassium channel reveals a putative binding site for general anesthetics. *ACS Chem. Neurosci.* **5,** 1246–1252 (2014).

33. Aicart-Ramos, C., Valero, R. A. & Rodriguez-Crespo, I. Protein palmitoylation and subcellular trafficking. *Biochim. Biophys. Acta - Biomembr.* **1808,** 2981–2994 (2011).

34. Herold, K. F., Sanford, R. L., Lee, W., Andersen, O. S. & Hemmings, H. C. Clinical concentrations of chemically diverse general anesthetics minimally affect lipid bilayer properties. *Proc. Natl. Acad. Sci. U. S. A.* 201611717 (2017). doi:10.1073/pnas.1611717114

35. Booker, R. D. & Sum, A. K. Biophysical changes induced by xenon on phospholipid bilayers. *Biochim. Biophys. Acta - Biomembr.* **1828,** 1347–1356 (2013).

36. Hemmings, H. C. *et al.* Emerging molecular mechanisms of general anesthetic action. *Trends Pharmacol. Sci.* **26,** 503–510 (2005).

37. Mlodzianoski, M. J. *et al.* Sample drift correction in 3D fluorescence photoactivation localization microscopy " Interferometric fluorescent super- resolution microscopy resolves 3D cellular ultrastructure. *Rev. Cell Dev. Biol. J. Opt. EXPRESS Proc. Natl. Acad. Sci. U.S.A. Protoc* **26,** 285–314 (2010).

38. Petersen, E. N., Chung, H. W., Nayebosadri, A. & Hansen, S. B. Kinetic disruption of lipid rafts is a mechanosensor for phospholipase D. *Nat. Commun.* **7,** 13873 (2016).

39. Kiskowski, M. A., Hancock, J. F. & Kenworthy, A. K. On the use of Ripley's K-function and its derivatives to analyze domain size. *Biophys. J.* **97,** 1095–1103 (2009).

40. Sengupta, P., Jovanovic-Talisman, T. & Lippincott-Schwartz, J. Quantifying spatial organization in point-localization superresolution images using pair correlation analysis. *Nat. Protoc.* **8,** 345–354 (2013).

41. Hartley, J. M. *et al.* Super-Resolution Imaging and Quantitative Analysis of Membrane Protein/Lipid Raft Clustering Mediated by Cell-Surface Self-Assembly of Hybrid Nanoconjugates. *ChemBioChem* **16,** 1725–1729 (2015).

42. Sengupta, P. *et al.* Probing protein heterogeneity in the plasma membrane using PALM and pair correlation analysis. *Nat. Methods* **8,** 969–975 (2011).

43. Patel, A. J. *et al.* Inhalational anesthetics activate two-pore-domain background K+ channels. *Nat. Neurosci.* **2,** 422–6 (1999).

ACKNOWLEDGEMENTS

We thank Andrew S. Hansen for assisting with experimental design and discussion and comments on the manuscript, Manasa Gudheti of Vutara for help with dSTORM data

processing, Michael Frohman for mPLD2 cDNA, and Guillaume Sandoz for chimeric TRAAK cDNAs. This work was supported by a Director's New Innovator Award (1DP2NS087943-01 to S.B.H.) from the NIH, a graduate fellowship from the Joseph B. Scheller & Rita P. Scheller Charitable Foundation to E.N.P. We are grateful to the Iris and Junming Le Foundation for funds to purchase a super-resolution microscope, making this study possible.

AUTHOR INFORMATION

[1]Department of Molecular Medicine, [2]Department of Neuroscience, The Scripps Research Institute, Jupiter, Florida 33458, USA.

[3]Department of Chemistry, The Scripps Research Institute, La Jolla, California 92037, USA

CONTRIBUTIONS

MAP, RAL, and SBH designed the experiments and wrote the manuscript. MAP performed all electrophysiology, dSTORM, and PLD2 enzymes assays with help from ENP for dSTORM imaging, and PLD2 assays.

COMPETING INTERESTS

The authors declare no competing interests.

MATERIALS & CORRESPONDENCE

shansen@scripps.edu

Figures and Figure Legends:

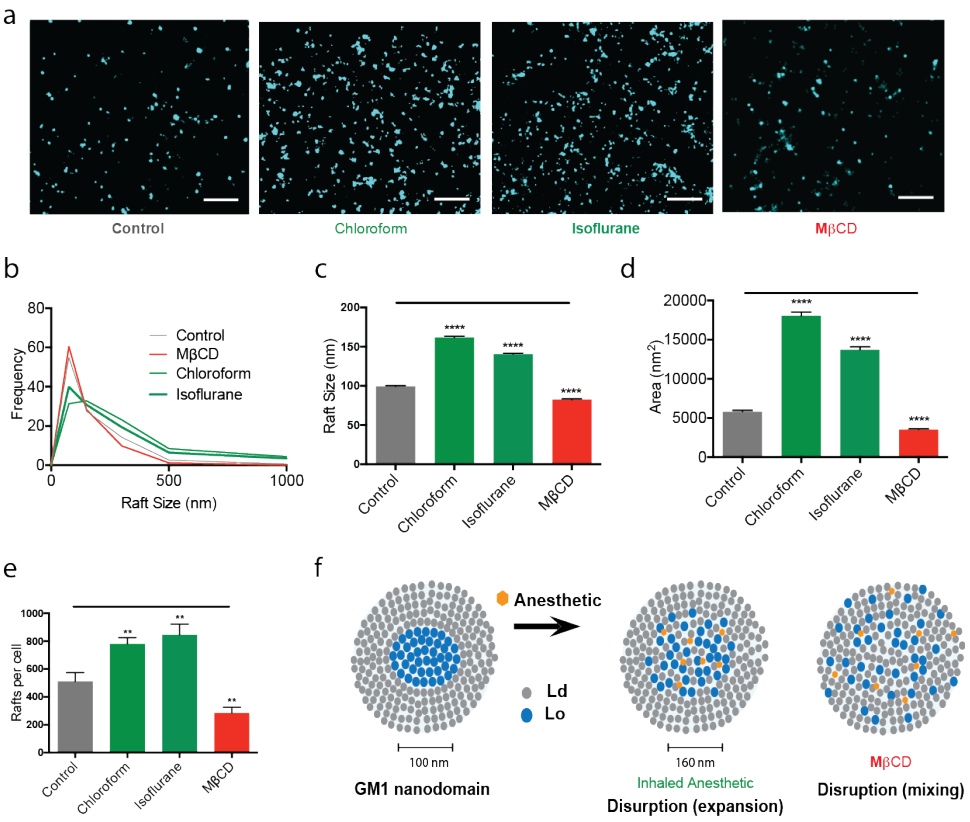

Figure 1 | Inhaled anesthetics disrupt GM1 domain structure. a, Representative reconstructed super-resolution (dSTORM) images of GM1 domains (lipid rafts) before and after treatment with chloroform (1 mM), isoflurane (1 mM), or MβCD (100 μM) (Scale bars: 1 μm). **b**, Frequency distribution of the GM1 domain size after anesthetic treatments (n=10). **c-d**, Bar graphs comparing the average sizes (**c**) and areas (**d**) quantified by cluster analysis (± s.e.m., n = 2842-7382). **e**, Quantified number of rafts per cell. (± s.e.m., n=10) (Student's t-test results: ****P<0.0001) **f**, Model representation of raft disruption by anesthetics. GM1 lipids (blue) form ordered domains of ~100 nm. Inhaled anesthetic (orange hexagon) intercalate and disrupt lipid order causing the domain to expand ~60% to 160 nm. MβCD depletes cholesterol inhibiting the formation of ordered domains causing the components to mix with the disordered lipids (grey).

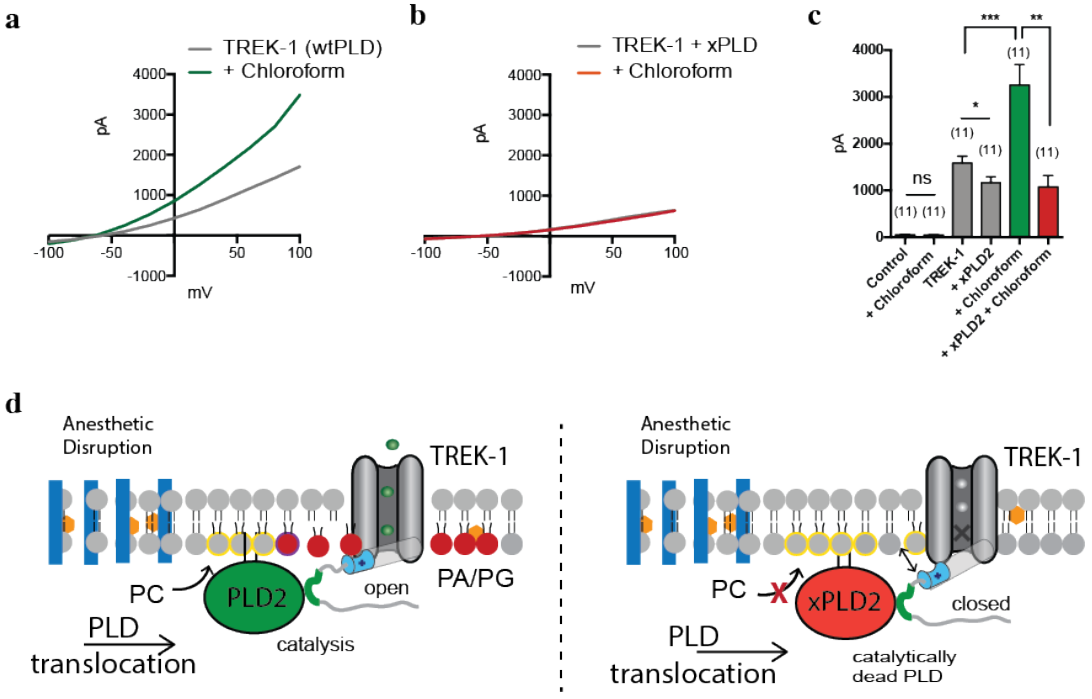

Figure 2 | Activation of TREK-1 by inhaled anesthetic is PLD2 dependent. a, Representative TREK-1 whole-cell currents activated by chloroform (1 mM) in physiological K^+ gradients. The current-voltage relationships (I-V curves) were elicited by 1-s depolarizing pulses from -100 to 100 mV in +20 mV increments. **b**, Representative I-V curves showing that co-expression of a catalytically inactive mutant of PLD2 (xPLD2 = PLD2_K758R) abolishes the TREK-1 activation by chloroform. **c,** Bar graph showing the ~2-fold increase of TREK1 current when activated by chloroform (1 mM) (n = 11) at +40 mV (± s.e.m.). **d,** Schematic representation of TREK-1 activation by inhaled anesthetics. Anesthetic disruption of GM1 domains causes PLD2 to localize with TREK-1 and its substrate phosphatidylcholine (PC) in the disordered region of the membrane. As PLD2 hydrolyzes PC to phosphatidic acid (PA), the anionic lipid binds to a known gating helix (grey cylinder), with a lipid binding site (cyan)[25], that activates TREK-1. Student's t-test results: *P < 0.05; **P<0.01; ***P<0.001; NS ≥ P.0.05.

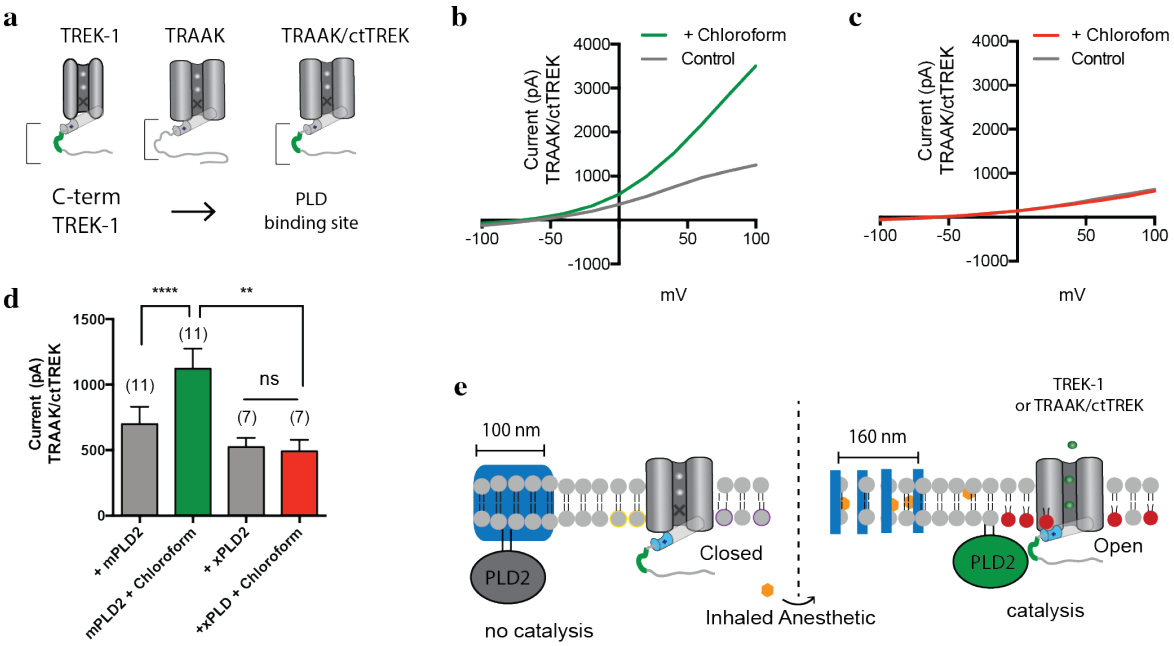

Figure 3 | PLD2 localization renders TRAAK anesthetic sensitive. Native TRAAK is an anesthetic insensitive channel. **a,** Cartoon showing experimental setup—TRAAK fused with the C-terminus of TREK-1 (TRAAK/ctTREK). **b-c**, Representative I-V curve showing TRAAK/ctTREK-1 is activated by chloroform when co-expressed with mouse PLD2 (mPLD2) (**b**) and the co-expression of the catalytically inactive PLD2 (xPLD2) abolishes the activation of TRAAK/ctTREK-1 chimeric channel by the chloroform (± s.e.m., n = 7) (**c**). **d,** Bar graph summarizing TRAAK/ctTREK-1 chimeric channel current in the presence or absence of xPLD2 and chloroform (1mM) at +40 mV (± s.e.m., n = 11) (Student's t-test results: ****P<0.0001, **P<0.01; NS ≥ P.0.05.) **e,** Model mechanism showing that anesthetics activate the TRAAKctTREK-1 chimeric channel through raft disruption and PLD2 substrate presentation; xPLD2 abolishes the activation (the color scheme is as in Fig. 2).

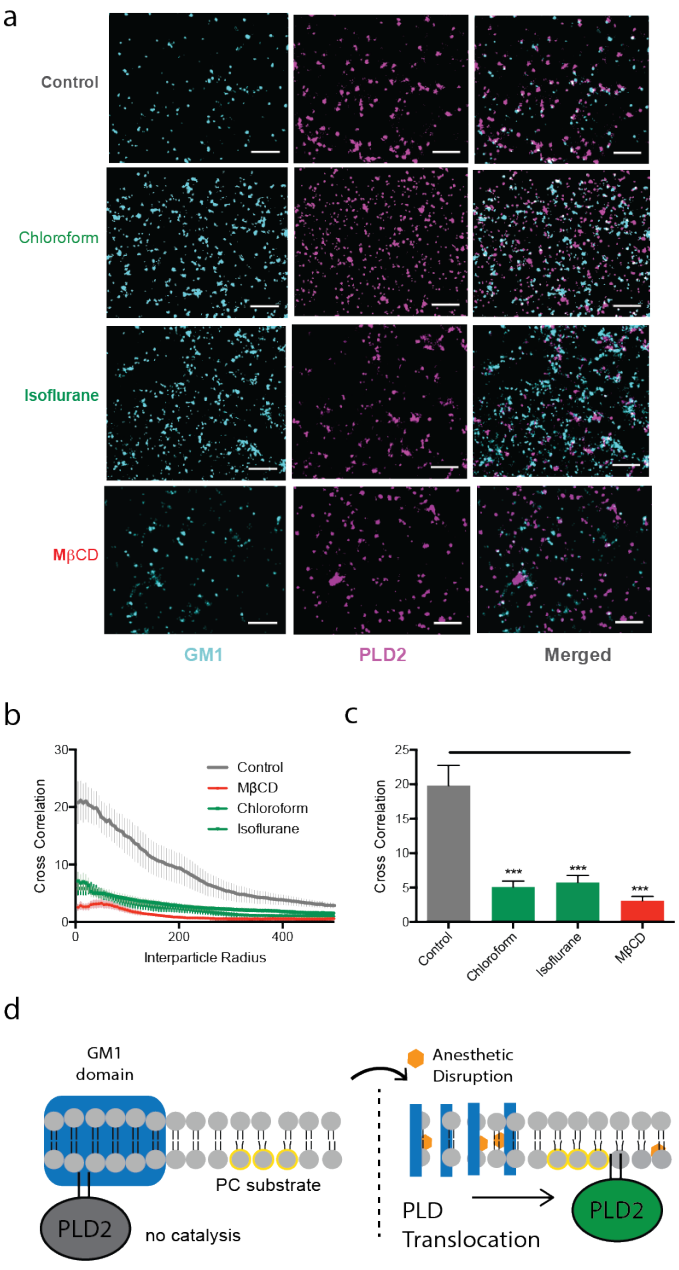

Figure 4 | Inhaled anesthetics displace PLD2 from GM1 domains. a, Representative super-resolution (dSTORM) images of fluorescently labeled CTxB (lipid raft) and PLD2 before treatment (Control) and after treatment with chloroform (1 mM), isoflurane (1mM), and MβCD (100 μM) in N2A (scale bars: 1 μm). **b**, Average cross-correlation functions (C(r)) showing a decrease in PLD2 association with ordered GM1 domains after treatment with anesthetic or

MβCD. **c**, Comparison of the first data point in (**b**) (5 nm radius) (± s.e.m., n = 10-17). **d**, Schematic representation of PLD2 in GM1 domain before (left) and after (right) anesthetic treatment. Palmitoylation drives PLD into GM1 domains (blue) away from its unsaturated PC substrate (yellow outline). Anesthetics (orange hexagon) disrupts GM-1 domains causing the enzyme to translocate where it finds its substrate PC in the disordered region of the cell.

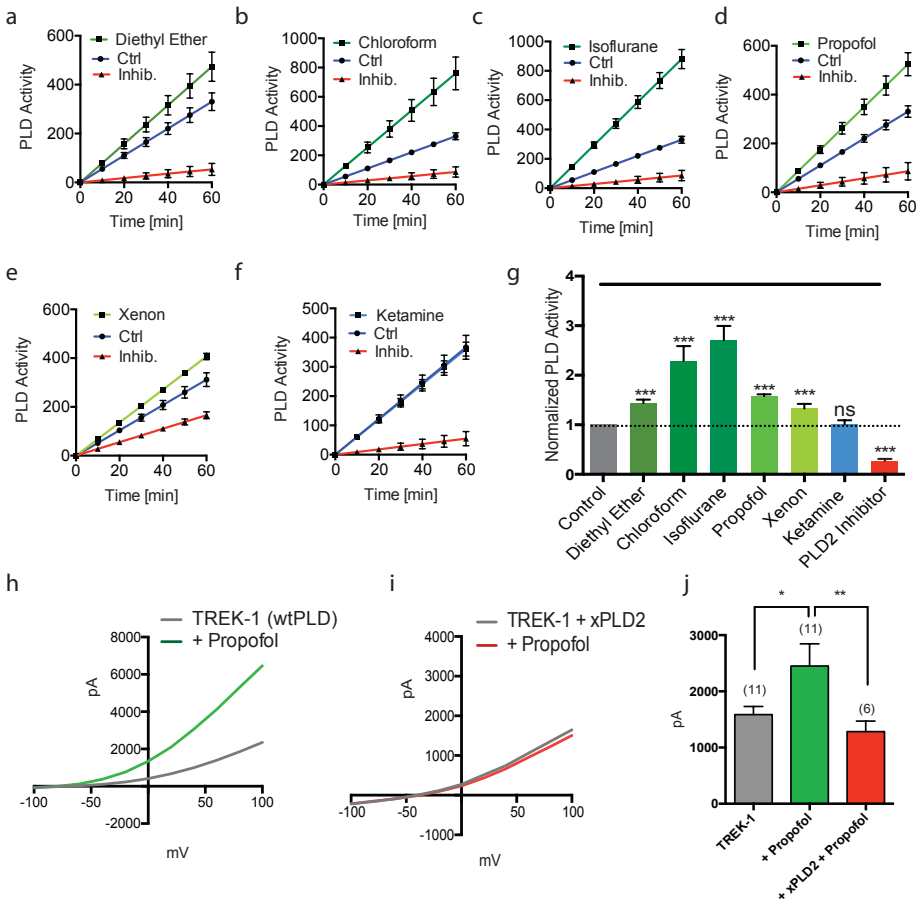

Figure 5 | General anesthetics activates phospholipase D2 (PLD2) through raft disruption. a-e, Live cell assays showing the effect of anesthetics on PLD2 activity in N2A cells. Chloroform (1 mM) (**a**), isoflurane (1 mM) (**b**), diethyl ether (1 mM) (**c**), propofol (50 μM) (**d**) and xenon (0.044 μM) (**e**) increased the PLD2 activity as compared with the control cells. Ketamine (50 μM) (**f**) had no effect on the PLD2 activity and the activity was inhibited by a PLD2 specific inhibitor (2.5-5 μM) (mean ± s.e.m., n = 4). **g**, Summary of normalized anesthetic induced activity of PLD2 in (a-f) at 60 min. (mean ± s.e.m., n = 4). **h-i,** Representative I-V curves) showing the effects of propofol on TREK-1 in HEK293 cells using whole cell patch clamp (**h**), and with xPLD2(**i**). **j,** Summary of TREK-1 currents showing an ~2 fold increase when activated by propofol (25-50 μM) (n = 6) at +40 mV (± s.e.m.).

SUPPLEMENTARY INFORMATION

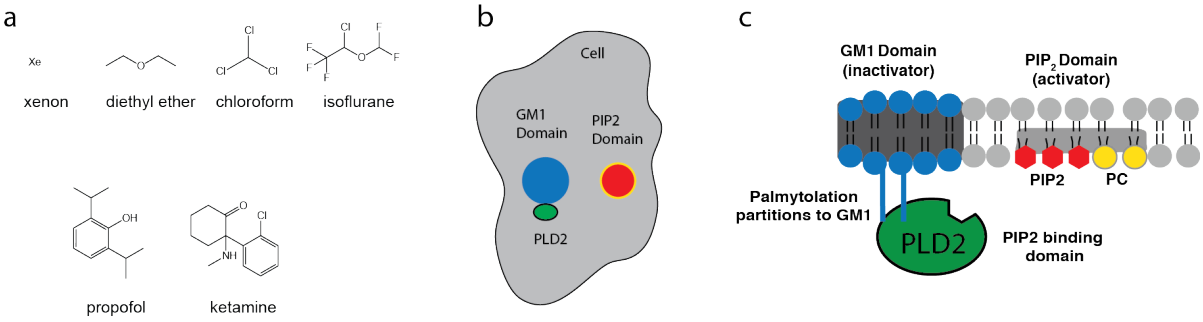

Supplementary Figure 1 | GM1 domains and PLD2 activation by substrate presentation. a, Chemical structures of general anesthetics are shown. Diversity ranges from xenon, a single hydrophobic atom, to ketamine a bicyclic small molecule. **b**, the organization of PLD2 and lipid rafts on the surface of a cell are shown (not to scale). GM-1 domains are comprised of GM1 saturated lipids and cholesterol, palmitoylation drives PLD2 into GM1 domains (blue circle) where it is sequestered away from its substrate polyunsaturated PC and PIP_2 domains (Red circle with yellow outline). **c**, Side view of the membrane in (**b**) with PLD2 localized to the inner leaflet through two palmitoylation sites (blue lines). GM1 domains also commonly referred to as the liquid ordered phase (Lo) are thicker than the liquid disordered phase (Ld). We previously showed mechanical force disrupts lipid rafts and causing PLD2 translocates to the PIP_2 domains. PLD2 has a PIP2 binding site and resides in equilibrium between GM1 domains and PIP_2 domains. PIP_2 is polyunsaturated and preferentially localized with unsaturated PC—PLD2 generates unsaturated PA and PG products through substrate presentation[15].

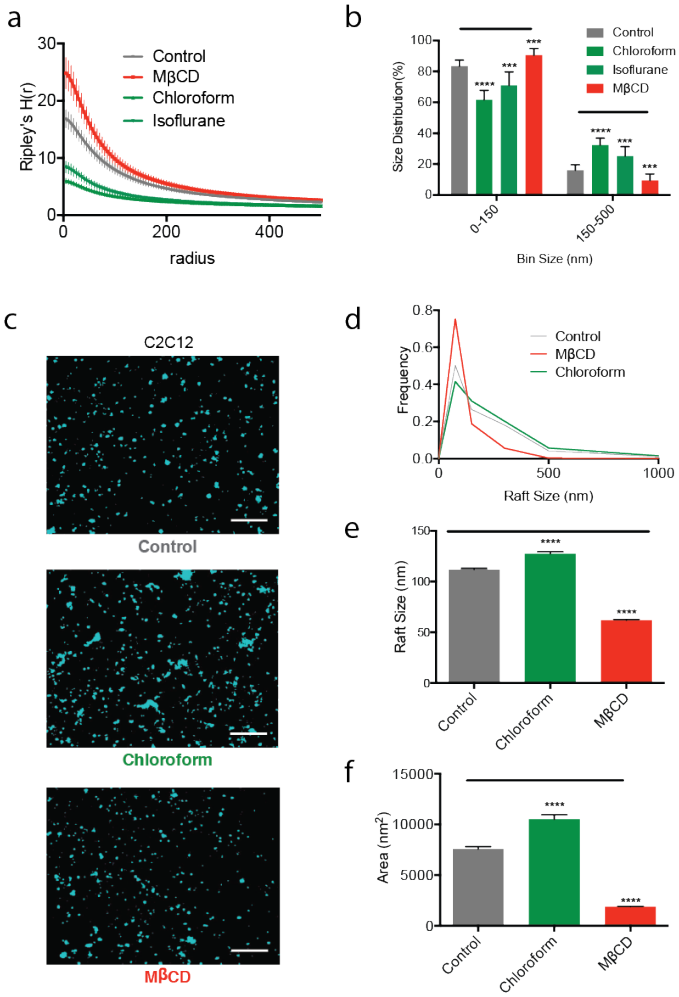

Supplementary Figure 2 | Inhaled anesthetics disrupt GM1 domains. a, Derivatives of Ripley's K-Function (H(r)) demonstrating the separation of GM1 domains with or without treatment of the inhaled anesthetics (1 mM) or MβCD (100 μM) (± s.e.m., n = 10). **b,** Histograms showing the size distribution of lipid rafts from N2A cells binned from 0-150 nm and 150-500 nm. Chloroform (1mM) and isoflurane (1mM) both shift from small to large and MβCD (100 μM) shifts from large to small (± s.e.m., n = 10). Both observations are a form of disruption. **c,** Representative super-resolution (dSTORM) images of lipid rafts from C2C12 cells before and after the treatment of the volatile anesthetics or MβCD (100 μM) (Scale bars: 1 μm). **d**, Particle

size distribution curve of the lipid rafts after the chloroform, isoflurane, and MβCD treatments from multiple C2C12 cells (n = 6-8). **e-f**, Bar graphs comparing the average lipid raft sizes (**e**) and areas (**f**) quantified by cluster analysis showing the disruption of lipid raft by chloroform and MβCD (± s.e.m., n = 2844-6525). Student's t-test results: ***P<0.001; ****P<0.0001.

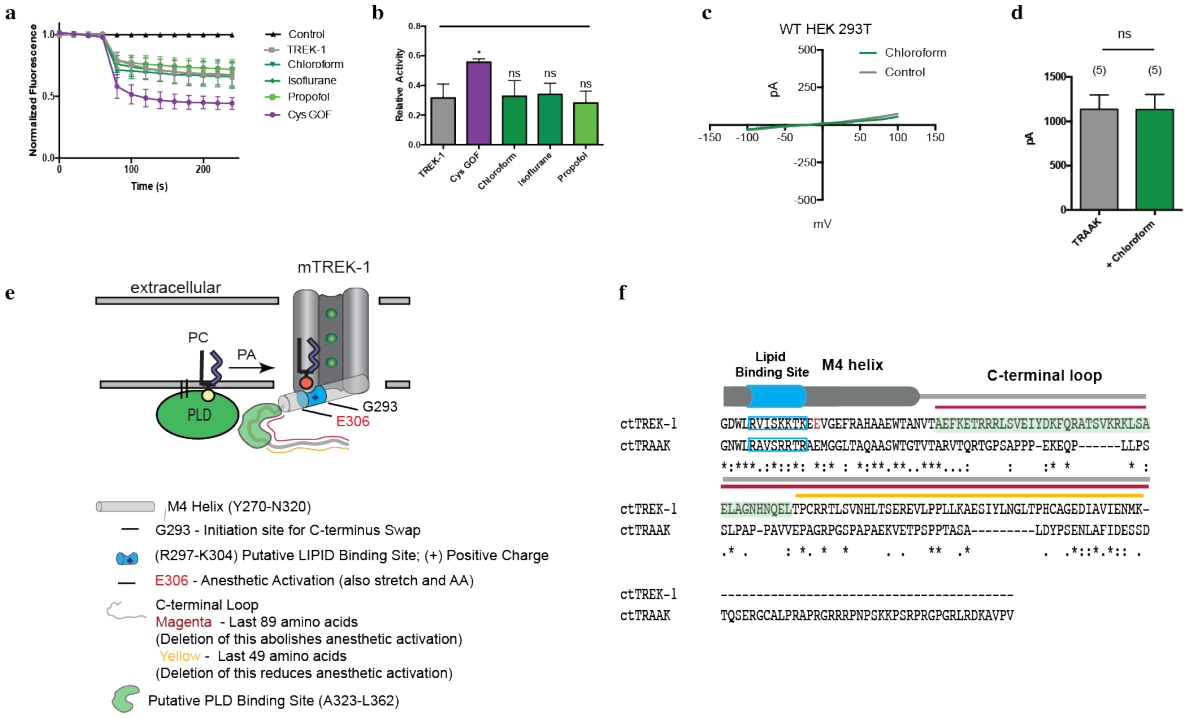

Supplementary Figure 3 | General anesthetics activate TREK-1 through PLD2. a, Ion flux assay of purified TREK-1 reconstituted into DOPC (16:1) liposomes with 15 mol% DOPG anionic lipid. Anesthetics chloroform (1 mM), isoflurane (1 mM), and propofol (50 μM) had no significant effect on channel currents compare to the double cysteine gain of function mutation (Cys GOF) (± s.e.m., n = 3-5). **b,** Bar graph comparing the relative activity from **e**. **c,** Current-voltage relationship (I-V) for TREK-1 in wild type HEK 293T. No change in whole cell currents by 1 mM of chloroform. **d,** Bar graph summarizing wt. TRAAK channel currents when activated by chloroform (1mM) at +40 mV (± s.e.m., n = 5) confirming a previous result that TRAAK is anesthetic insensitive. **e**, Cartoon depicting the amino acids that are known to play a role in anesthetic activation and the PLD2 dependent lipid gating of TREK-1 channels. **f,** multiple-sequence alignment between the swapped C-terminus of mouse TREK-1 (293-411) and TRAAK (255-398) generated with Clustal Omega (EMBL-EBI).

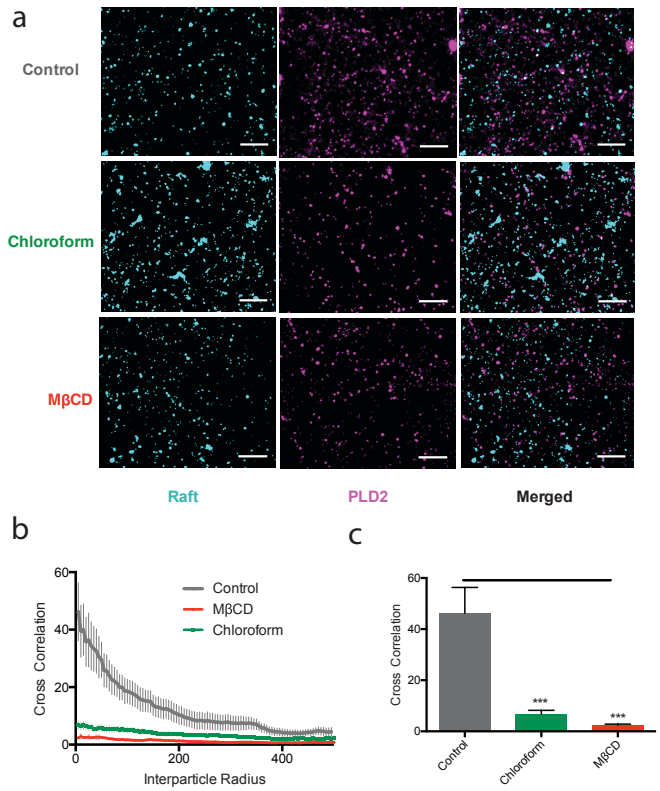

Supplementary Figure 4 | Inhaled anesthetics displace PLD2 from GM1 domains in C2C12 cells. a, Representative super-resolution (dSTORM) images of fluorescently labeled lipid raft (CTxB) and PLD2 before and after the treatment with chloroform (1 mM), and MβCD (100 μM) in C2C12 cells (Scale bars: 1 μm). **b-c**, Average Cross-correlation functions (C(r)) (**b**) and the function normalized at C(r=5) (**c**) shows chloroform (1 mM) and MβCD (100 μM), disrupt PLD2 localization into lipid raft in C2C12 cells (± s.e.m., n = 5). Student's t-test results: *P < 0.05; ***P<0.001; ****P<0.0001; NS ≥ P.0.05.

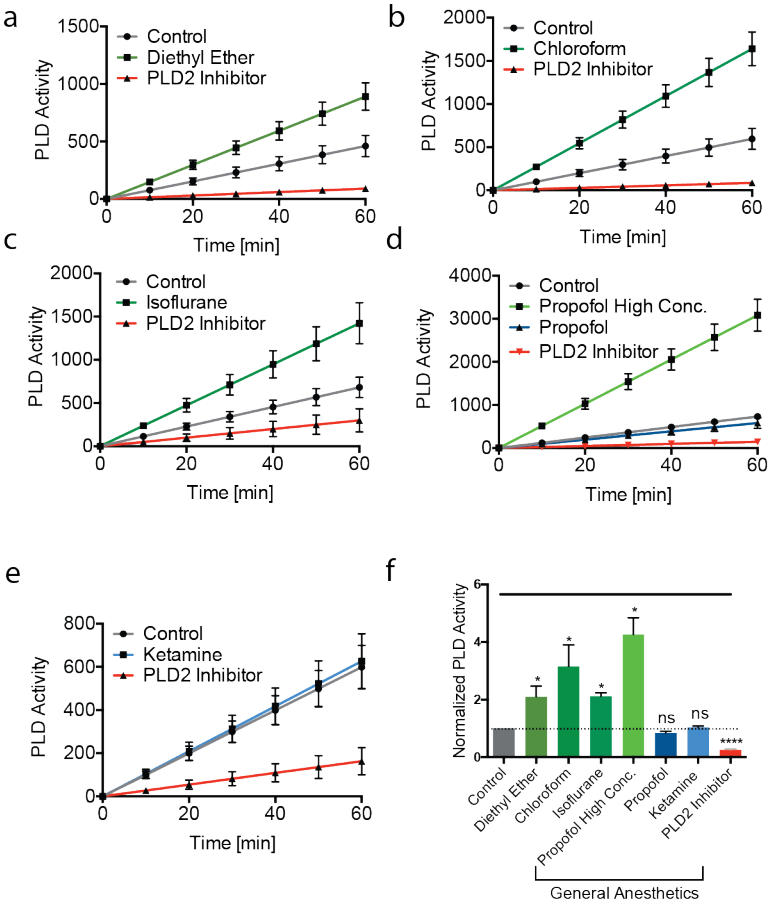

Supplementary Figure 5 | Activation of PLD2 by general anesthetics in C2C12 cells. a-e, Diethyl ether (1 mM) (**a**), chloroform (1 mM) (**b**), isoflurane (1 mM) (**c**), and higher concentration of propofol (400 μM), but not 50 μM propofol (**d**) (green lines) activate PLD2 compared to control cells. Ketamine (50 μM, blue line) had no observed effect on PLD2 activity. (**e**) PLD2 inhibitor (2.5-5 μM) inhibited the activity (± s.e.m., n = 4). **f**, Normalized summary effect of anesthetics on PLD2 activity at 60 min from the above experiments (± s.e.m., n = 4). Student's t-test results: *P < 0.05; ***P<0.001; ****P<0.0001; NS ≥ P.0.05.

Methods

Sample preparation for Super Resolution Microscopy (d-STORM)

Super Resolution Microscopy was performed on C2C12 cells. Confluent cells were first differentiated overnight with serum-free DMEM in 8-well chamber slides (Nunc Lab-Tek Chamber Slide System, Thermo Scientific). Cells were then washed and treated with anesthetics or other drugs for 10 min. Chambers containing volatile anesthetic were tightly sealed with aluminum stickers. Cells were then chemically fixed with 3% paraformaldehyde and 0.1% glutaraldehyde in PBS for 10 min at room temperature with shaking, and the fixing solution was quenched by incubating with 0.1% $NaBH_4$ for 7 min followed by three times 10 min wash with PBS. Anesthetics or the drugs were also added into the fixing solution to ensure its effect on the cell. Fixed cells were then permeabilized with 0.2% Triton-X 100 in PBS for 15 min except the cells receiving the CTxB treatment. Cells were blocked using a standard blocking buffer (10% BSA, 0.05% Triton in PBS) for 90 min at room temperature. Cells were labeled with the primary antibody with appropriate dilutions (anti-PLD2 antibody (Sigma) 1:500 dilution; CTxB (Life Technologies) 1:1000 dilution) in the blocking buffer for 60 min at room temperature. Cells were then extensively washed with 1% BSA, 0.05% Triton in PBS for five times 15 min each before labeling with the secondary antibody diluted into the blocking buffer and incubating for 30 min. Prior to labeling, the secondary antibody was conjugated to either Alexa 647 (to detect CTxB raft) or Alexa 555 (to detect PLD2 or TREK1). The incubation with secondary antibody was followed by above extensive wash and a single 5 min wash only with PBS. Labeled cells were then post-fixed with the previous fixing solution for 10 min without shaking followed by three times 5 min washes with PBS and two 3 min washes with deionized distilled water. To elucidate the lipid raft disruption by anesthetics or other drugs, compounds were applied to the reaction buffer at these concentrations: chloroform (1 mM) (Fisher

Scientific); isoflurane (1 mM) (Sigma); mβCD (100 μM) (Fisher); diethyl ether(1mM) (Sigma); ketamine (50 μM) (Cayman Chemicals); xenon (Praxair).

d-STORM Image Acquisition and Analysis

Imaging was performed with A Zeiss Elyra PS1 microscope using TIRF mode equipped with an oil-immersion 63X objective. Andor iXon 897 EMCCD camera was used along with the Zen 10D software for image acquisition and processing. The TIRF mode in the dSTORM imaging provided low background high-resolution images of the cell membrane harboring lipid microdomains. A total of 15,000 frames with an exposure time of 18 ms were collected for each acquisition. Excitation of the Alexa Fluor 647 dye was achieved using 642 nm lasers and Alexa Fluor 555 was achieved using 561 nm lasers. Cells were imaged in a photo-switching buffer suitable for dSTROM: 1% betamercaptoethanol, 0.4 mg glucose oxidase and 23.8 μg Catalase (oxygen scavengers), 50 mM Tris, 10 mM NaCl, and 10% glucose at pH 8.0. Sample drift during the acquisition was corrected for by an autocorrelative algorithm[37] or tracking several immobile, 100 nm gold fiducial markers using the Zen 10D software. The data were filtered to eliminate molecules with localization precisions >50 nm.

Super-resolved Images were constructed using the default modules in the Zen Software. Each detected event was fitted to a 2D Gaussian distribution to determine the center of each point spread function (PSF) plus the localization precision. The Zen software also has many rendering options including the options to remove the localization errors, outliers in brightness and size. The super-resolved images have an arbitrary pixel size of 16 nm. To determine the raft size determination and the cross-correlations, the obtained localization coordinates were converted to be compatible to Vutara SRX software (version 5.21.13) by an Excel macro. Cross-correlation and raft size estimation were calculated through cluster analysis using the

default analysis package in the Vutara SRX software[38–41]. Cross-correlation function $c(r)$ estimates the spatial scales of co-clustering of two signals – the probability of localization of a probe to distance r from another probe[42]. Raft sizes are the size of clusters determined by measuring the area of the clusters comprising of more than 10 observations.

In Vivo PLD2 activity measurements

A nonradioactive method was performed to measure in vivo PLD2 activity as described previously (ref) (Fig. S2). Briefly, C2C12 cells were seeded into 96-well flat culture plates with transparent-bottom to reach confluency (~ 5 x 104 per well). Then the confluent cells were differentiated with serum-free DMEM for a day and washed with 200 µL of phosphate buffer saline (PBS). The PLD assay reactions were promptly begun by adding 100 µL of working solution with or without anesthetics. The working solution contained 50 µM Amplex red, 1 U per ml horseradish peroxidase, 0.1 U per ml choline oxidase, 30 µM dioctanoyl phosphatidylcholine (C8PC), and 20mM Glucose in PBS. Anesthetics were directly dissolved into the working buffer from freshly made stocks and incubated overnight before assay reagents were added. In case of volatile anesthetics, 96-well plates were tightly sealed with aluminum sticky films after adding the reaction buffer. The PLD activity and the background (lacking cells) was determined in triplicate for each sample by measuring fluorescence activity with a fluorescence microplate reader (Tecan Infinite 200 PRO, reading from bottom) for 2 hours at 37°C with at excitation wavelength of 530 nm and an emission wavelength of 585 nm. Subsequently, PLD activity was normalized by subtracting the background and to the control activity. Data were then graphed (Mean ± SEM) and statistically analyzed (student t-test) with GraphPad Prism software (v6.0f).

Electrophysiology

Whole cell patch clamp recordings of TREK1 currents were made from TREK-1-transfected HEK 293T cells as described previously (lab ref, Comoglio et. al. 2014). Briefly, HEK 293T were

cultured in growth media [DMEM, 10% heat-inactivated fetal bovine serum, 1% penicillin/ streptomycin] in a humidified incubator (95% air and 5% CO_2) at 37°C. When the HEK 293T cells were ~90% confluent, they were seed at 50% confluency per 35-mm dish containing 15mm glass coverslips coated with poly-D-lysine (1 mg/ml) to ensure good cell adhesion. The cells were then transiently transfected using X-tremeGENE (Sigma) with a total of 1µg of DNA per dish. For co-transfection of TREK1, TRAAK with PLD2 or PLD2-K758R cells were transfected with a ratio of 1:3. Human TREK1 pCEH and mouse PLD2 was kindly provided by Dr. Stephen B. Long, Sloan Kettering Institute, NY. TRAAK/Ct-TREK1 (starting at Gly 293) pIRES2eGFP and TREK1/Ct-TRAAK (starting at Gly 255) pIRES2eGFP was kindly provided by Dr. Sandoz Guillaume, iBV CNRS, Université de Nice Sophia Antipolis, France. HEK 293T cells were obtained from ATCC (Manassas, VA). Human TRAAK was a gift from Dr. Steve Brohawn, University of California, Berkeley. Transfected cells were then visualized and selected for electrophysiology 24-48 hours post transfection using green fluorescent protein. Standard whole-cell currents were recorded at room temperature with Axopatch 200B amplifier and Digidata 1440A (Molecular Devices) and measured with Clampex 10.3(Molecular Devices) at sample rate of 10 kHz and filtered at 2 kHz. The recording micropipettes were made from the Borosilicate glass electrode pipettes (B150-86-10, Sutter Instrument) by pulling with the Flaming/Brown micropipette puller (Model P-1000, Sutter instrument). The micropipette resistances were ranged from 3-7 MΩ and filled with the internal solution (in mM): 140 KCl, 3 $MgCl_2$, 5 EGTA, 10 HEPES, 10 TEA pH 7.4 (adjusted with KOH). The external bath solution contained (in mM): 145 NaCl, 4 KCl, 2 $CaCl_2$, 1 $MgCl_2$, 10 HEPES, 10 TEA pH 7.4 (adjusted with NaOH). After the voltage offset was adjusted to zero current between the patch electrode and the bath solution, the whole cell configuration was achieved by repetitive gentle suctions on cells sealed at 1-10 GΩ. In the whole cell configuration, cells were held at −60 mV and currents were elicited by voltage steps command (at -100 to +100 mV from V_{hold} = -60 mV) and voltage ramp commands (-100 mV to +50 mV in 5 ms). Volatile anesthetic, chloroform, was

applied using a gravity-driven (5 ml/min) gas-tight perfusion systems (Valves and tubing were made of PTFE). HEK 293T cells were perfused with control solution or the test solution that contained the volatile anesthetic. Chloroform was dissolved based on the anesthetic saturation experiments that it has 66.6 mM solubility in water at 37°C[43]. Subsequently, data were replayed and analyzed using Clampfit 10 (Molecular Devices) to generate current-voltage relationship (I-V Curve) from voltage steps protocol. Student's *t*-test was applied to assess statistical significance using Prism6 (GraphPad software) and judged significant at $p < 0.001$. The values represented in the graphs are Mean ± SEM.

Chanel Purification and Flux Assay

TREK-1 channel protein purification and Flux assay were done as previously described[24,25]. Briefly, Pichia yeast was used to express zebrafish TREK-1 (1-322 amino acids) containing GFP at C-terminus. Followed by cryo milling, the extraction of the proteins were done in dodecyl-β-d-maltoside (DDM) with protease inhibitors. The proteins were then purified on a cobalt affinity column to homogeneity followed by size exclusion chromatography (SEC). The final SEC buffer contained 20 mM Tris (pH 8.0), 150 mM KCl, 1 mM EDTA, and 2 mM DDM. All proteins were collected with a predominant monodispersed peak corresponding to the expected molecular weight (MW) of the assembled channel protein plus GFPs. This Purified TREK-1 was used to generate Proteoliposomes by mixing 1:100 TREK-1/lipids. The ratio of the Lipids (85% DOPC and 15% DOPG) were mixed, dried, and solubilized in rehydration buffer (150 mM KCl, 20 mM HEPES [pH 7.4]) and calibrated with 3 mM DDM before the channel mixing. DDM was then removed by BioBeads (Bio-Rad) and the proteoliposomes (5 µL) were sonicated and added to 195 µL of flux assay buffer (150 mM NaCl, 20 mM HEPES [pH 7.4], 2 µM 9-amino-6-chloro-2-methoxyacridine [ACMA]) in a 96-well plate at room temperature. Flux was initiated by the addition of the protonophore carbonyl cyanide m-chlorophenyl hydrazone (CCCP) (3.2 µM).